The Journal of Immunology

RESEARCH ARTICLE | FEBRUARY 03 2023

First-in-Human Study in Healthy Subjects with the Noncytotoxic Monoclonal Antibody OSE-127, a Strict Antagonist of IL-7Rα

Nicolas Poirier; ... et. al

J Immunol ji2200635.
https://doi.org/10.4049/jimmunol.2200635

First-in-Human Study in Healthy Subjects with the Noncytotoxic Monoclonal Antibody OSE-127, a Strict Antagonist of IL-7Rα

Nicolas Poirier,*[,1] Irène Baccelli,*[,1] Lyssia Belarif,* Riad Abès,* Géraldine Teppaz,* Caroline Mary,* Sonia Poli,[†] Claudia Fromond,* Isabelle Girault,* Sabrina Pengam,* Emilienne Soma,* Fanny De Sa,* Jean-Pascal Conduzorgues,* Cécile Braudeau,[‡,§] Regis Josien,[‡,§] Bram Volckaert,[¶] Dominique Costantini,* and Frédérique Corallo*

OSE-127 is a humanized mAb targeting the IL-7Rα-chain (CD127), under development for inflammatory and autoimmune disease treatment. It is a strict antagonist of the IL-7R pathway, is not internalized by target cells, and is noncytotoxic. In this work, a first-in-human, phase I, randomized, double-blind, placebo-controlled, single-center study was carried out to determine the safety, pharmacokinetics, pharmacodynamics, and immunogenicity of OSE-127 administration. Sixty-three healthy subjects were randomly assigned to nine groups: six single ascending dose groups with i.v. administration (0.002–10 mg/kg), a single s.c. treatment group (1 mg/kg), and two double i.v. injection groups (6 or 10 mg/kg). Subjects were followed during <146 d. OSE-127's pharmacokinetic half-life after a single dose increased from 4.6 (1 mg/kg) to 11.7 d (10 mg/kg) and, after a second dose, from 12.5 (6 mg/kg) to 16.25 d (10 mg/kg). Receptor occupancy was ≥95% at doses ≥0.02 mg/kg, and this saturation level was maintained >100 d after two i.v. infusions at 10 mg/kg. IL-7 consumption was inhibited by OSE-127 administration, as demonstrated by a decreased IL-7 pathway gene signature in peripheral blood cells and by ex vivo T lymphocyte restimulation experiments. OSE-127 was well tolerated, with no evidence of cytokine-release syndrome and no significant alteration of blood lymphocyte counts or subset populations. Altogether, the observed lack of significant lymphopenia or serious adverse events, concomitant with the dose-dependent inhibition of IL-7 consumption by target cells, highlights that OSE-127 may show clinical activity in IL-7R pathway–involved diseases. ***The Journal of Immunology*****, 2023, 210: 1–11.**

Interleukin-7 is a limiting cytokine that is constitutively produced by stromal cells in nonhematological tissues (such as the lungs, skin, and intestine), as well as by lymphoid tissues (bone marrow and thymus), and by lymphatic endothelial cells (1–3). It is required for the ontogeny of T cells and lymphoid structures and is needed to maintain their survival, proliferation, and immune homeostasis (3–5). More specifically, IL-7 is key for the generation of memory T cells (6, 7) and the long-term maintenance of $CD4^+$ and $CD8^+$ central and effector memory T cells (8–11). It also stimulates cytotoxic activity of $CD8^+$ T cells (12), imprints some tissue-homing specificity on T cells (13, 14), and can act via $CD4^+$ T cells and monocytes to increase B cell activation (15).

IL-7 signals through cell surface IL-7R, which comprises two subunits: the IL-7Rα-chain (CD127) and the common cytokine receptor IL-7Rγ-chain (CD132, γ_c, IL-2RG) (16). The heterodimerization of CD127 with CD132 is required for IL-7–induced signaling. More specifically, IL-7 interacts with domain D1 of CD127 (site 1) and domain D1 of CD132 (site 2a); in addition, CD127 and CD132 interact together through their D2 domains (site 2b), stabilizing and forming an active IL-7/CD127/CD132 ternary complex (17, 18). Upon activation, IL-7R delivers proliferative and antiapoptotic signals, primarily by activating the JAK-STAT pathway and inducing the expression of the antiapoptotic protein BCL-2 (2, 4, 19). CD127 is also a component of the thymic stromal lymphopoietin (TSLP) receptor and is required for competent TSLP signaling (20).

Naive and even more so memory T lymphocytes express high levels of CD127, whereas naturally occurring regulatory T cells (Tregs) express low levels of CD127 (21). This differential expression constitutes a unique opportunity to selectively target pathogenic effectors while preserving natural regulators. Indeed, high expression of the IL-7/IL-7R pathway associates with numerous diseases (22), including among others inflammatory bowel diseases (13, 23), type 1 diabetes (24, 25), rheumatoid arthritis (26–28), psoriasis (29), primary Sjögren's syndrome (30, 31), acute lymphoblastic leukemia (32–36), and multiple sclerosis (37, 38). Additionally, genome-wide studies revealed genetic variants of IL-7R associating with autoimmune diseases (39, 40). Based on these observations, strategies that target IL-7R have been developed for the treatment of IL-7R pathway deregulated diseases (13, 41–43).

OSE-127 is a humanized IgG4 mAb that binds site 1 and site 2b of CD127, thereby preventing the heterodimerization and subsequent activation of IL-7R, without impacting TSLP receptor signaling (44). It is an IgG4 Fc isotype comprising the S228P hinge mutation, which prevents Fab-arm exchange (45). Importantly, OSE-127 stands out

*OSE Immunotherapeutics, Nantes, France; [†]Poli Consulting, Geneva, Switzerland; [‡]CHU Nantes, Laboratoire d'Immunologie, Centre d'Immunomonitorage Nantes Atlantique, Nantes, France; [§]CHU Nantes, Nantes Université, INSERM, CR2TI UMR 1064, Nantes, France; and [¶]SGS Life Sciences, Clinical Pharmacology Unit, Antwerp, Belgium

[1]N.B. and I.B. contributed equally to this work as first authors.

ORCIDs: 0000-0001-9842-2372 (S.P.); 0000-0003-0885-9381 (C.F.); 0000-0002-9587-5197 (I.G.); 0000-0002-3367-8059 (J.-P.C.); 0000-0001-7900-7413 (R.J.); 0000-0001-7967-2915 (B.V.).

Received for publication August 25, 2022. Accepted for publication January 11, 2023.

This work was supported by Bpifrance Effimab Grant I 1302011W.

The RNA-seq data presented in this article have been submitted to the Gene Expression Omnibus under accession number GSE224046.

Address correspondence and reprint requests to Dr. Frederique Corallo, OSE Immunotherapeutics, 22 Boulevard Benoni Goullin, 44200 Nantes, France. E-mail address: frederique.corallo@ose-immuno.com

The online version of this article contains supplemental material.

Abbreviations used in this article: ADA, anti-drug Ab; AUC, area under the curve; BMI, body mass index; C_{max}, maximum concentration; MAD, multiple ascending dose; PD, pharmacodynamic; PK, pharmacokinetic; qPCR, quantitative PCR; RNA-seq, RNA sequencing; RO, receptor occupancy; SAD, single ascending dose; sCD127, soluble CD127; ssGSEA, single-sample gene set enrichment analysis; TEAE, treatment-emergent adverse event; Treg, regulatory T cell; TSLP, thymic stromal lymphopoietin.

from previously developed anti–IL-7R mAbs by its absence of Ab-induced receptor internalization (41, 46), its lack of Ab-dependent or complement-dependent cytotoxic activity (32, 43, 44), and its lack of agonist activity on IL-7/IL-7R signaling (41, 44). OSE-127 preclinical studies illustrated its strict antagonist property in the control of graft-versus-host disease or colitis in humanized mice (13) as well as in the inhibition of pathogenic memory T cell reactivation in ex vivo colon explant cultures from inflammatory bowel disease (13) or Sjögren's syndrome patients (47). Similarly, OSE-127 (but not partially agonist and antagonist anti–IL-7R mAbs targeting the site 1 epitope only) induced long-term control of memory T cell–dependent skin inflammation in nonhuman primates (44).

In this study, to our knowledge, we report the first-in-human administration of OSE-127 through single and multiple ascending i.v. and s.c. doses to characterize its safety, pharmacokinetics, pharmacodynamics, and immunogenicity in healthy subjects.

Materials and Methods

Study design

This study is a first-in-human, phase I, randomized, double-blind, placebo-controlled, single-center study evaluating single and multiple ascending i.v. and s.c. doses of OSE-127 in healthy subjects. It was approved by the Ziekenhuisnetwerk Antwerpen Independent Ethics Committee (protocol no. OSE-127-C101; EudraCT no. 2018-001832-22; ClinicalTrials.gov identifier NCT03980080). The study was conducted at SGS Life Science Services, Clinical Pharmacology Unit Antwerp, Antwerp, Belgium, in compliance with Good Clinical Practice guidelines, with the principles of the Declaration of Helsinki, and in line with European guidelines for first-in-human clinical trials (EMEA/CHMP/SWP/28367/07 rev.1).

Participants

Eligible male and female subjects gave written informed consent. Key inclusion criteria were general good health, 18–65 y of age, a weight of at least 50 kg and not exceeding 100 kg, with a body mass index (BMI) of 19–30 kg/m^2. Exclusion criteria were any significant past medical history or abnormal laboratory tests.

Interventions

The test drug was OSE-127 (supplied by the sponsor, OSE Immunotherapeutics, Nantes, France), whereas the comparator drug (matching placebo) was a 20 mM histidine acetate (pH 5.5), 180 mM sorbitol, 50 mM glycine, and 0.02% (w/w) Tween 20 solution. OSE-127 was supplied as 2-ml extractable volume vials containing 100 mg of OSE-127 (50 mg/ml) in 20 mM histidine acetate (pH 5.5), 180 mM sorbitol, 50 mM glycine, and 0.02% (w/w) Tween 20.

Reconstitution of the study drug to adjust the concentration before administration was performed on the site pharmacy by appropriate dilutions in NaCl 0.9% solution. The sponsor provided a manual with detailed instructions for study drug preparation to the site. The study drug was prepared by the SGS pharmacy in accordance with this manual. The pharmacy staff used the randomization list to prepare both the study drug and the placebo, which were stored below −60°C and provided to the investigator in a double-blind manner.

The doses were initially selected based on population pharmacokinetic (PK)-pharmacodynamic (PD) modeling of nonhuman primate data (with allometric adaptation), and emerging data from the single-dose groups in part 1 of the study were later included to define the dosing interval in double-dose groups of part 2. The initial dose (minimal anticipated biological effect level, 0.002 mg/kg) corresponded to a modeled CD127 receptor occupancy (RO) at a maximum concentration (C_{max}) of ∼20%. Based on exposure and clinical observations from the GLP toxicology study in monkeys, the maximal dose was determined at 10 mg/kg.

For dose levels ≤0.2 mg/kg, OSE-127 was administered by i.v. infusion of 10 ml for at least 15 min, after dilution to the correct concentration. For other dose levels, OSE-127 was administered by i.v. infusion of 100 ml during at least 60 min, after dilution to the correct concentration. The dose in cohort B was administered s.c. by injection of a maximal volume of 4 ml (two separate injections of maximal 2 ml each) after dilution to the right concentration.

Treatment regimens

In part 1, 47 subjects were selected in two different cohorts (cohort A for single ascending dose [SAD] with six groups of 39 subjects in total and cohort B with 8 additional subjects) and 16 subjects in part 2 (multiple ascending dose [MAD]; see Table I). For each treatment period, subjects were housed at the study center from the day before dosing (day −1) until the morning of day 3 in parts 1 and 2 as well as from the evening of day 13 until the morning of day 16 for the second dosing in part 2. An interval of at least 14 d (last to first administration) was applied between all dose levels to allow a Safety Committee to review the cumulative safety and PK/RO data from previous dose levels before proceeding to the next dose level.

Part 1: SAD. Cohort A enrolled 39 subjects in one of the six i.v. dose-level groups: 0.002 mg/kg in group 1, 0.02 mg/kg in group 2, 0.2 mg/kg in group 3, 1 mg/kg in group 4, 4 mg/kg in group 5, and 10 mg/kg in group 6. In groups 1–3, five subjects were randomized to either OSE-127 or placebo in a 3:2 ratio so that three subjects received OSE-127 and two received placebo. In groups 4–6, eight subjects were randomized to either OSE-127 or placebo in a 6:2 ratio so that six received OSE-127 and two received placebo. A total of eight subjects were enrolled in cohort B, all comprised within group 7: the subjects were randomized to either OSE-127 or placebo administered s.c. in a 6:2 ratio so that six subjects received OSE-127 and two received placebo.

Part 2: MAD. In part 2, 16 subjects were enrolled in one of the two dose level groups (8 in each group): 6 mg/kg in group 8 and 10 mg/kg in group 9. Each subject received two administrations of OSE-127 or placebo separated by an interval of 14 d.

Cytokine assessment

Blood samples were collected predose and postdose at hours 4 and 96 (day 5) for the SAD cohort only. Cytokines IFN-γ, TNF-α, IL-4, IL-5, IL-6, IL-8, and IL-12p70 were assayed in serum using a human 7-plex Milliplex kit (no. HCYTOMAG-60K-07: IL-4, IL-5, IL-6, IL-8, IL-12p70, IFN-γ, and TNF-α, Merck Millipore, Molsheim, France) and quantified using a Luminex MAGPIX instrument (Luminex, Austin, TX). All experiments were performed by the BioAnalytical Laboratory of Nantes University Hospital (Centre d'Immunomonitorage de Nantes Atlantique, Nantes, France), and results were analyzed by OSE Immunotherapeutics (Nantes, France).

IL-7 and soluble CD127 measurement in serum

IL-7 and soluble CD127 (sCD127) measurement was carried out in groups 1–6 (SAD cohort) at predose and postdose: 4 h, 8 d, and 57 d after OSE-127 or placebo administration. Briefly, for dosage of human IL-7, a human IL-7 Quantikine immunoassay (Bio-Techne, Minneapolis, MN, no. HS750) was used to measure IL-7 concentration in human sera. The quantitative sandwich enzyme immunoassay technique was employed. A mAb specific for human IL-7 (Bio-Techne, no. 890193) was precoated onto a microplate. Standards and samples were captured by the immobilized Ab. After washing, an enzyme-linked polyclonal Ab specific for human IL-7 (Bio-Techne, no. 890194) was added to the wells. Following washing, a substrate solution was added to the wells. After an incubation period, an amplifier solution was added, and OD at 490 nm with a wavelength correction at 650 or 690 nm was measured by a spectrophotometer reader (Tecan, Männedorf, Switzerland). For dosage of human soluble IL-7Rα-chain (sCD127), anti-CD127 clone human IL-7R-M21 Ab (BD Biosciences, no. 552853, which does not compete with OSE-127 for binding to CD127) was precoated onto a standard Multi-Array MSD microplate. To determine total sCD127, standards and samples were spiked with an excess of OSE-127 (1 μg/ml final) and captured by the immobilized Ab. To determine the amount of sCD127/OSE-127 complexes, only standards were spiked with an excess of OSE127 (1 μg/ml). After washing, the sCD127/OSE-127 complexes were revealed with an anti-human IgG4-SULFO-TAG Ab (Thermo Fisher Scientific, Waltham, MA, no. MA5-16716). Following washing, reading buffer was added to the wells and luminescence was measured on an MSD reader.

PK analysis

Serial blood samples for PK assessment were collected at the following time points relative to infusion start time within both SAD and MAD parts: predose and postdose at hours 0.5, 0.75, 1, 2, 4, 8, 12, and 24 (day 2) and at days 3, 5, 8, 15, 29, 43, and 57 and every other 2 wk until the last follow-up visit of each dose level, when all subjects of the group had reached a RO ≤20%. Concentrations of OSE-127 in serum were determined by a qualified vendor (SGS Lab, Poitiers, France) using a validated ELISA-like electrochemiluminescence immunoassay/Meso Scale Discovery method on an MSD Sector Imager 6000 (MSD, Gaithersburg, MD). The laboratory analysis was carried out following the principles of Good Laboratory Practice regulations of the Organization for Economic Cooperation and Development by SGS Lab (Poitiers, France) using Phoenix WinNonlin 6.2 or higher (Pharsight, Palo Alto, CA). The lower limit of quantification and the upper limit of quantification for OSE-127 during the intrarun and interrun evaluations were determined as 31.3 and 2000 ng/ml, respectively. The mean precision (percent coefficient of variation) was <17.00% and the mean accuracy was within

91.35–102.62%. A standard curve was constructed, enabling sample concentrations to be estimated by interpolation from the fitted curve.

PD analysis

Blood samples were collected at the same time points as PK analyses for IL-7 RO (CD127 RO), using a fit-for-purpose validated flow cytometry assay carried out by a qualified vendor (SGS Lab, Poitiers France). Free receptors on cell surface were measured by using a competitive Ab of the test item and, in parallel, the total amount of receptors available was determined using a noncompetitive Ab. Abs used were as follows: Pacific Blue mouse anti-human CD3, clone SP34-2, BD Biosciences (no. 558124), PE mouse anti-human CD127, clone HIL-7R-M21 (noncompeting Ab, to determine total CD127), BD Biosciences (no. 557938), and Alexa Fluor 647 mouse anti-human CD127, clone A019D5 (competing Ab, to detect free CD127), BioLegend (no. 351318). CD127 occupancy by OSE-127 on subject blood cells was then calculated for each subject by performing the ratio between the percent positive cells or the mean fluorescence intensity of the cell population of interest. Intradonor replicate precision and interdonor precision were inferior to 30% (coefficient of variation).

Peripheral T lymphocyte subpopulations and activation status were assessed by flow cytometry on whole blood. Blood samples were harvested at t0 and days 15 and 57 after i.v. infusion in the SAD cohort, part 1 and at *t*0 and days 8, 22, and 30 after the first i.v. administration in the MAD cohort and then immediately frozen in CryoStor CS10 freezing solution (Biolife Solutions, STEMCELL Technologies, Grenoble, France) as previously described (48). Samples were thawed and stained for CD45, CD3, CD45RA, CD4, CD8, CD25, CD27, CD28, PD1, and CCR7 markers with DURAClone T cell tubes (Beckman Coulter, Roissy, France) to define the following subpopulations: naive T cells, activated T cells, memory T cells, central memory T cells, effector memory T cells, and resting effector memory T cells, in the $CD4^+$ and $CD8^+$ compartments. Natural Tregs were also recorded using DURAClone Treg tubes (Beckman Coulter) containing Abs to CD45, CD3, CD4, CD25, and FOXP3 with the addition of CD127-allophycocyanin-R700 Ab (clone human IL-7R-M21, BD Biosciences, Le Pont De Claix, France). Samples were analyzed using a CytoFLEX flow cytometer (Beckman Coulter) by the BioAnalytical Laboratory (Centre d'Immunomonitorage de Nantes Atlantique, Nantes, France) and analyzed by OSE Immunotherapeutics (Nantes, France).

Standard laboratory tests were performed by the ZNA Middelheim laboratory (Antwerp, Belgium).

The potential effect of OSE-127 on IL-7 consumption by blood cells was investigated ex vivo, monitored through evaluation of the IL-7–induced prevention of T cell apoptosis. Briefly, human PBMCs from healthy subjects were harvested at day 3 after a single i.v. administration of OSE-127 or placebo and were cultured ex vivo with autologous serum (also harvested at day 3). Research-grade human recombinant IL-7 (Miltenyi Biotec, Bergisch Gladbach, Germany, no. 130-095-367) was added at different concentrations (5, 20, or 50 ng/ml) and, after homogenization, PBMCs were cultivated for 12 d. Analysis of live cells per well at day 12 of culture was performed by flow cytometry (LSR II, BD Biosciences, Franklin Lakes, NJ) using the cell proliferation dye eFluor 450 (eBioscience, San Diego, CA, no. 65-0842-85, batch 1979389) and the following Abs, following the manufacturer's instructions: FITC-labeled anti–annexin V (BD Biosciences, no. 556419, batch 7209930), PE-labeled anti-human CD3 (BD Biosciences, no. 555340, batch 8162560, clone HIT3a), allophycocyanin-labeled anti-human CD45RA (BD Biosciences, no. 550855, batch 8029741, clone HI100), and PE-Cy5–labeled anti-human CD25 (BD Biosciences, no. 555433, batch 412964, clone M-A25).

Immunogenicity assessment

Blood samples for anti–OSE-127 Ab detection were collected in both SAD and MAD parts at screening and on day 1 (predose), days 15, 29, 43, and 57, and every other week up to day 141. The titration of anti–OSE-127 Abs (anti-drug Ab [ADA]) in serum was performed using a validated electrochemiluminescence immunoassay. The method used an acidic treatment of the serum samples to allow, when necessary, dissociation of OSE-127/ADA followed by a single-step assay bridging format whereby ADAs are captured in solution by a combination of biotinylated and SULFO-TAG–labeled forms of OSE-127. Complex formation was subsequently detected by ECL on the MSD platform. Using sCD127 IgG4 (human IL-7RA/CD127 protein [His/Fc tag]) supplied from Sino Biological and purchased from Interchim (no. 10975-H03H) as a positive control, the sensitivity level of the assay was 1.00 ng/ml and the mean drug tolerance was 3.53 μg/ml at the sensitivity level.

Statistical analysis

No formal power calculation was performed to determine sample size because this study did not aim to test a statistical hypothesis, but rather aimed to explore safety, tolerability, and PK of a new molecule for the first time in humans while exposing a minimum number of subjects. Based on precedent sets by other phase I studies similar in design, a sample size of 63 healthy volunteers was deemed sufficient to meet the objectives of the protocol. All statistical calculations were performed by SGS LS using the SAS (SAS Institute, Cary, NC; version 9.4 or higher) software for statistical computations and for graphical purposes. WinNonlin Phoenix 8.0 (Pharsight, Palo Alto, CA) was used for calculations of PK and PD parameters.

RNA sequencing analyses

For IL-7 signature identification on ex vivo–treated human PBMCs, RNA sequencing (RNA-seq) results are accessible in the Gene Expression Omnibus under the accession number GSE103643 (https://www.ncbi.nlm.nih.gov/geo/query/acc.cgi?acc=GSE103643), and the methods for data generation were previously reported (44).

OSE-127 signature RNA-seq data are accessible in the Gene Expression Omnibus under accession number GSE224046. For OSE-127 signature identification on in vivo–treated human PBMCs, a total of 48 blood samples were collected in Paxgen tubes: 22 samples were drawn preadministration of OSE-127 (10 mg/kg) or placebo, 22 paired samples were collected on day 15 after administration, and 4 paired samples were collected on day 57. One sample did not pass quality control and was removed from the study. RNA with rRNA and globulin depletion was 150-bp end sequenced on an Illumina HiSeq by Genewiz (Chelmsford, MA). Raw fastq files were quality checked by FastQC. Reads were pseudoaligned to CRGh38/hg38 using Salmon with the index preparation option genecode, and raw counts, as well as normalized TPM reads for each gene, were generated using Salmon with the option geneMap. Pseudo mapping quality reads were evaluated using FastQC, with an average of 20–30 million reads with >90% bases ≥30 for all samples.

DESeq2 was used for differential gene expression analysis with the raw count table from Salmon using the DESeq2_1.30.0 package in R version 4.0.3 (2020-10-10). The analysis used time point and patient ID in the study design to compare two time points for each paired samples (design = ~Screening_number + Time). Genes with a Benjamin–Hochberg-adjusted p value <5% and fold change >1 were considered as differentially expressed. Subsequently, single-sample gene set enrichment analysis (ssGSEA) scores were computed using the GSVA R package based on the ssGSEA method (by setting the "ssgsea.norm" parameter to TRUE), as previously described (49, 50).

Reverse transcription–quantitative PCR

Reverse transcription with the SuperScript i.v. VILO master mix with ezDNASE (Thermo Fisher Scientific, Waltham, MA, no. 11766050) was performed to obtain cDNA with a DNase treatment to eliminate genomic DNA. TaqMan Fast advanced master mix (5 ml; Thermo Fisher Scientific, no. 4444557) and TaqMan probes were used on a ViiA 7 real-time analyzer to quantify each gene and housekeeping genes. The sum of the $-\Delta Ct$ normalized to the TBP housekeeping gene was calculated and used as a signature.

Results

Participant flow

The study was conducted in a single clinical center from November 30, 2018 to November 4, 2019. A total number of 63 subjects was divided over two study parts (Table I): a SAD study (part 1) and a MAD study (part 2). In part 1, cohort A, 27 subjects were administered a single i.v. dose of OSE-127 (ranging from 0.002 to 10 mg/kg, groups 1–6), and 12 subjects were administered a single i.v. dose of placebo.

Table I. Treatment regimens

	Dose (mg/kg)	OSE-127 (45 subjects)	Placebo (18 subjects)
Part 1, cohort A, single ascending dose (i.v.)			
Group 1	0.002	3	2
Group 2	0.02	3	2
Group 3	0.2	3	2
Group 4	1	6	2
Group 5	4	6	2
Group 6	10	6	2
Part 1, cohort B, single ascending dose (s.c.)			
Group 7	1	6	2
Part 2, multiple ascending dose (i.v.)			
Group 8	6	6	2
Group 9	10	6	2

In part 1, cohort B, six subjects were administered a single s.c. dose of OSE-127 (1 mg/kg, group 7) and two subjects were administered a single s.c. dose of placebo. In part 2, 12 subjects were administered two i.v. doses of OSE-127 (6 or 10 mg/kg, groups 8 and 9, respectively), and 4 subjects were administered two i.v. doses of placebo, separated by an interval of 2 wk. A sentinel dose approach was applied for each group, that is, two subjects were dosed, followed by the remaining subjects of the group 24 h later (total 2 d). One of the two subjects of day 1 was randomized to receive placebo.

All subjects in part 1 and part 2 received the study drug or placebo according to the randomization list. They all completed the study and were included in the safety analysis. The blinding code was not broken by the investigator or the sponsor for any of the subjects included in the study.

Baseline data

Subject demographics are shown in Table II. All subjects' age, weight, and BMI fell within the inclusion criteria defined in the protocol. Overall, the data did not differ meaningfully between the two different arms in both parts. The flow of assessments at screening and day −1 is shown in Supplemental Table I.

Safety

No death, other serious adverse event, or treatment-emergent adverse event (TEAE) leading to study discontinuation occurred during the study. All TEAEs reported in part 1 and 2 of the study were of grades 1 or 2 in severity (Table III).

No remarkable differences or dose-dependent trends in adverse event incidence could be observed between the different doses of OSE-127 and placebo, or between i.v. and s.c. administration of OSE-127. In part 1, 22 subjects (56.4%) of cohort A and 3 subjects (37.5%) of cohort B experienced at least one TEAE, which was considered as treatment-related for 13 (33.3%) subjects of cohort A and 1 subject of cohort B. In part 2, 11 subjects (68.8%) experienced at least one TEAE, with treatment-related TEAEs reported in 5 (31.3%) subjects. In both parts, the most frequently reported treatment-related TEAE was headache (nine subjects [23.1%] in cohort A and three subjects [18.8%] in part 2).

No remarkable difference or dose-dependent trend in laboratory values over time could be observed between the several OSE-127 doses and placebo or between i.v. and s.c. administration of OSE-127 in part 1 or 2. Most treatment-emergent laboratory abnormalities were observed in one or two subjects per group.

In parts 1 and 2, changes over time in vital signs and electrocardiogram parameters were generally small, and no clinically relevant no dose-dependent trends or differences with placebo were apparent.

Table II. Subject demographics at baseline

	Placebo	Total OSE-127
Safety population	18	45
Sex, *n* (%)		
Female	12 (67)	32 (71)
Male	6 (33)	13 (29)
Age (y)		
Mean (SD)	50 (8)	49 (12)
Median	53	53
Range	29–59	22–65
Race, *n* (%)		
White	18 (100)	45 (100)
Asian	0 (0)	0 (0)
Black/African American	0 (0)	0 (0)
BMI (kg/m^2)		
Mean (SD)	25 (2)	25 (3)
Median	25	25
Range	21–30	20–30

Pharmacokinetics

Fig. 1A illustrates the OSE-127 concentration-time data for all dose groups. Despite a nonsignificant dose proportionality of area under the curve $(AUC)_\tau$ observed in cohort A (groups 1–6, i.v. administration, OSE-127 0.002–10 mg/kg doses), an increase of dose-normalized AUC_τ was measured between 0.02 and 1 mg/kg, whereas dose-normalized AUC_τ seemed stable between 4 and 10 mg/kg, altogether indicative of a target-mediated drug disposition process at lower doses. Terminal elimination half-life increased from 111 to 280 h over the dose range of 1–10 mg/kg in single administration up to 300 and 390 h after the second dose of OSE-127 at 6 and 10 mg/kg respectively. Approximate dose proportionality for C_{trough}, C_{max}, AUC_{last}, and AUC_τ was observed after two i.v. infusions of OSE-127 from 6 to 10 mg/kg (part 2, groups 8 and 9). The accumulation ratio was ∼1.50 for AUC_τ and ∼1.25 for C_{max}.

Pharmacodynamics

Dose-dependent CD127 RO on peripheral T lymphocytes was observed after OSE-127 infusion. Following a single administration, CD127 was quickly saturated with RO ≥95% at the first sampling time after the end of infusion (0.5 h) from the dose of 0.02 mg/kg (Fig. 1B). CD127 RO area under the effect (versus time curve over the dosing interval) increased with ascending single i.v. doses from 0.02 to 10 mg/kg, and the median duration of CD127 RO >95% (t_{abl}) and >20% (t_{Emin}) was longer for higher doses. The same trend was observed after multiple i.v. doses (MAD part). CD127 RO area under the effect increased with ascending OSE-127 AUC_{last} and AUC_τ. Importantly, CD127 expression over time measured by flow cytometry on peripheral T lymphocytes (Fig. 2A) was stable after the administration of OSE-127, thus confirming that the mAb does not induce the internalization of IL-7R. Total lymphocyte counts monitored throughout the study remained within the physiological range, thus confirming that the mAb does not induce depletion of T cells (Fig. 2B). More specifically, flow cytometry analysis indicated that $CD3^+$ (Fig. 2C), $CD4^+$ (Fig. 2D), and $CD8^+$ (Fig. 2E) T cell frequencies were maintained following OSE-127 administration. Furthermore, no significant alteration was observed in the frequencies of effector, central, effector memory, and naive cells, neither in the CD8 (Fig. 3) nor in the CD4 compartments (Fig. 4).

In addition, monitoring of cytokine levels (TNF-α, IFN-γ, IL-12p70, IL-8, IL-6, IL-5, and IL-4) in the serum of participating subjects following both single and double administrations of OSE-127 demonstrated no significant impact on cytokine levels with no clinically relevant elevation of their levels (Fig. 5A–G).

Exploratory biomarker assessment detected an increase in IL-7 serum levels 4 h after single i.v. administration of OSE-127 at doses ≥0.2 mg/kg (Fig. 5H). Furthermore, an increase in sCD127 serum levels was measured 8 d after single i.v. administration of OSE-127 at doses ≥1 mg/kg (Fig. 5I). Both increases were reversible and consistent with the elimination pattern of OSE-127. The detected increase in IL-7 levels is most likely due to a decrease of IL-7 consumption by IL-7R, owing to OSE-127's antagonist activity. Further dissection of sCD127 level analysis revealed that only sCD127 complexed with OSE-127 (sCD127/OSE-127) but not free sCD127 increased in subjects' sera (Supplemental Fig. 1). Once complexed to OSE-127, the elimination pattern of sCD127 thus became similar to that of OSE-127. TSLP levels in the serum of subjects were below detection limits. Altogether, these results are in line with the current knowledge of the biology of interleukin pathways (51) and highlight IL-7 and sCD127 as reliable biomarkers for in vivo monitoring of OSE-127 activity.

Table III. Summary of TEAEs per treatment in part 1 (cohort A and B) and part 2

Part 1 (SAD), Cohort A								
Group (OSE-127 dose)	Placebo	Group 1 (0.002 mg/kg)	Group 2 (0.02 mg/kg)	Group 3 (0.2 mg/kg)	Group 4 (1 mg/kg)	Group 5 (4 mg/kg)	Group 6 (10 mg/kg)	All OSE-127–Treated Subjects
Number (%) with at least one TEAE	5 (41.7)	2 (66.7)	2 (66.7)	3 (100)	4 (66.7)	4 (66.7)	2 (33.3)	17 (62.9)
Serious TEAE	0	0	0	0	0	0	0	0
Treatment-related TEAE	2 (16.7)	0	2 (66.7)	2 (66.7)	4 (66.7)	2 (33.3)	1 (16.7)	11 (40.7)
TEAE leading to study drug discontinuation	0	0	0	0	0	0	0	0
Most frequently reported TEAEs overall (>1 subject)								
Headache	1 (8.3)	0	2 (66.7)	1 (33.3)	2 (33.3)	3 (50.0)	1 (16.7)	9 (33.3)
Nasopharyngitis	1 (8.3)	1 (33.3)	0	0	2 (33.3)	0	0	3 (11.1)
Diarrhea	0	0	1 (33.3)	1 (33.3)	1 (16.7)	0	0	3 (11.1)
Nausea	1 (8.3)	0	0	0	1 (16.7)	0	0	1 (3.7)

Part 1 (SAD), cohort B		
Group (OSE-127 dose)	Placebo	Group 7 (1 mg/kg)
Number (%) with at least one TEAE	1 (50.0)	2 (33.3)
Serious TEAE	0	0
Treatment-related TEAE	0	1 (16.7)
TEAE leading to study drug discontinuation	0	0

Part 2 (MAD)				
Group (OSE-127 dose)	Placebo	Group 8 (6 mg/kg)	Group 9 (10 mg/kg)	All OSE-127–Treated Subjects
Number (%) with at least one TEAE	3 (75.0)	4 (66.7)	4 (66.7)	8 (66.7)
Serious TEAE	0	0	0	0
Treatment-related TEAE	1 (25.0)	1 (16.7)	3 (50.0)	4 (33.3)
TEAE leading to study drug discontinuation	0	0	0	0
Most frequently reported TEAEs overall (>1 subject)				
Headache	1 (25.0)	2 (33.3)	2 (33.3)	4 (33.3)

Immunogenicity

Anti–OSE-127 Abs (ADAs) were detected after single (i.v. and s.c.) and multiple (i.v.) administration from a dose of 0.2 mg/kg and higher (Supplemental Tables II–IV). ADAs appeared during the elimination phase of OSE-127, and their occurrence was delayed with increasing and repeated doses, starting from 1 mo after the first administration for the lower single doses to almost 3 mo for the highest repeated dose. In most positive subjects, ADAs were detected

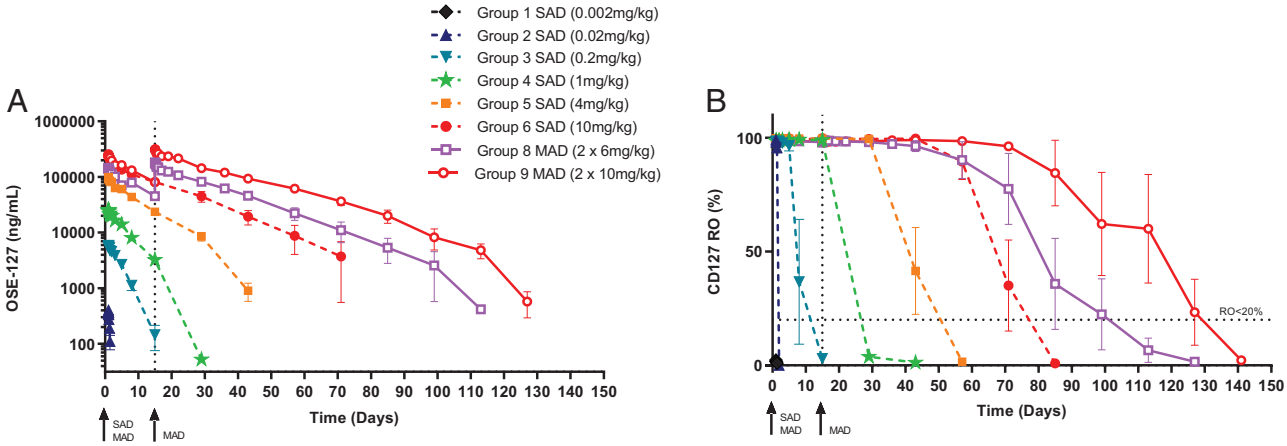

FIGURE 1. Pharmacokinetic and pharmacodynamic data. (**A**) Mean serum OSE-127 concentrations ± SEM (semilog scale) from predose to end of study. Single ascending dose (SAD) treatment groups (dashed lines) and multiple ascending dose (MAD) groups (plain lines) are displayed with $n = 3–6$ subjects per treatment group. (**B**) Mean CD127 receptor occupancy (RO) ± SEM across the OSE-127 treatment groups indicated in (A) from predose to end of study. $n = 3–6$ subjects per treatment group. Assessment of RO in subjects dosed with placebo resulted in a background signal ranging from 0 to 5%.

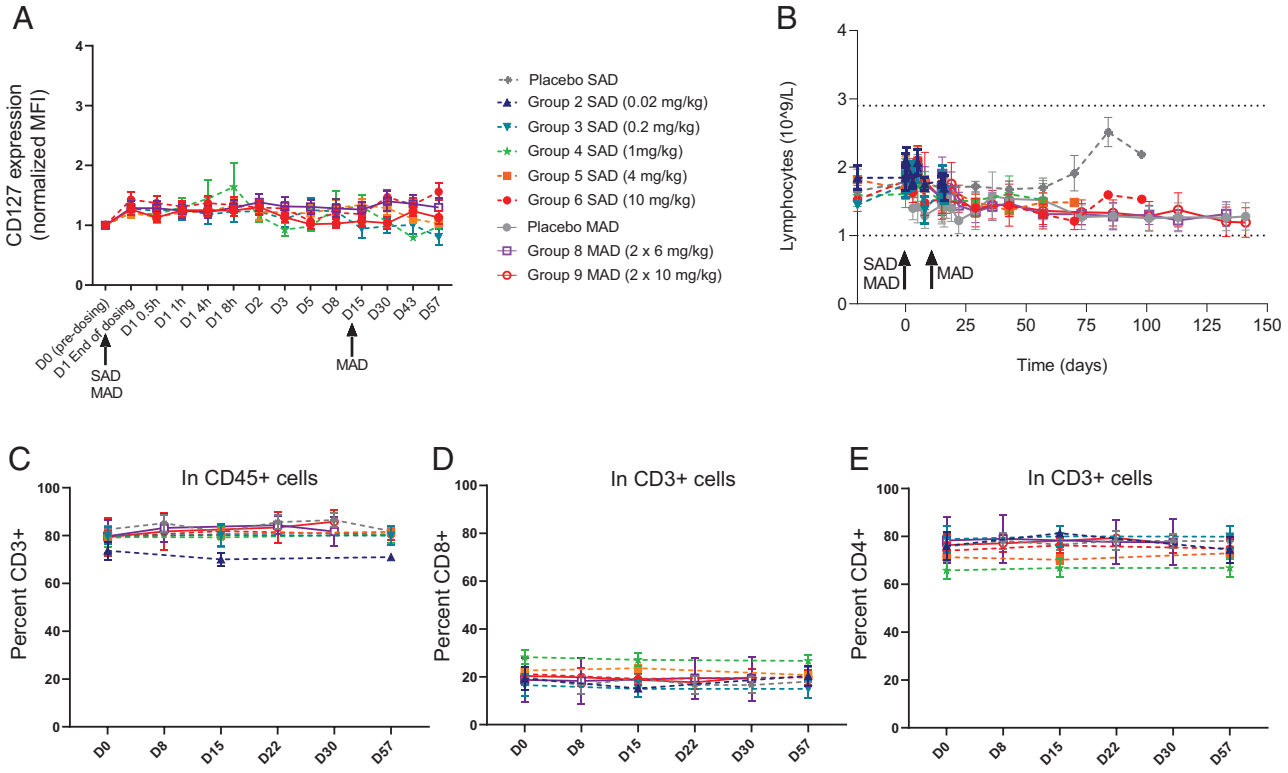

FIGURE 2. CD127 expression and lymphocyte monitoring in the blood of treated subjects. (**A**) CD127 expression (mean fluorescence intensity [MFI]) in the MAD cohort, normalized to pre-first dose evaluation. (**B**) Total lymphocyte counts throughout the study. (**C**) Frequencies of T lymphocytes assessed by flow cytometry. (**D** and **E**) Frequencies of CD8 T cells (D) and CD4 T cells (E) as indicated. Symbols refer to the groups defined in (A), and data are means ± SEM of $n = 3–6$ subjects.

for the first time once the elimination of OSE-127 had been almost complete (e.g., for 70% of the single-dose subjects once the concentration of OSE-127 in the blood was below the lower limit of detection of 31.3 ng/ml).

No validated assay was available for the assessment of the neutralizing potential of these ADAs. However, the comparison between individuals with ADAs and individuals without ADAs showed on average a similar clearance of the drug as well as similar RO values.

Ex vivo dose-dependent functional activity of OSE-127

IL-7–induced prevention of T cell apoptosis was next measured on ex vivo cultures of T lymphocytes isolated from the blood of treated subjects on days 0 and 3 after i.v. infusion of OSE-127 or placebo. PBMCs were cultured for 12 d with increasing doses of rIL-7 (0–50,000 pg/ml) and cells were stained with the annexin V apoptotic marker. Single administration of OSE-127 in healthy volunteers markedly and dose-dependently prevented IL-7–mediated T cell survival, more efficiently so in effector ($CD45RA^-$) than in naive ($CD45RA^+$)

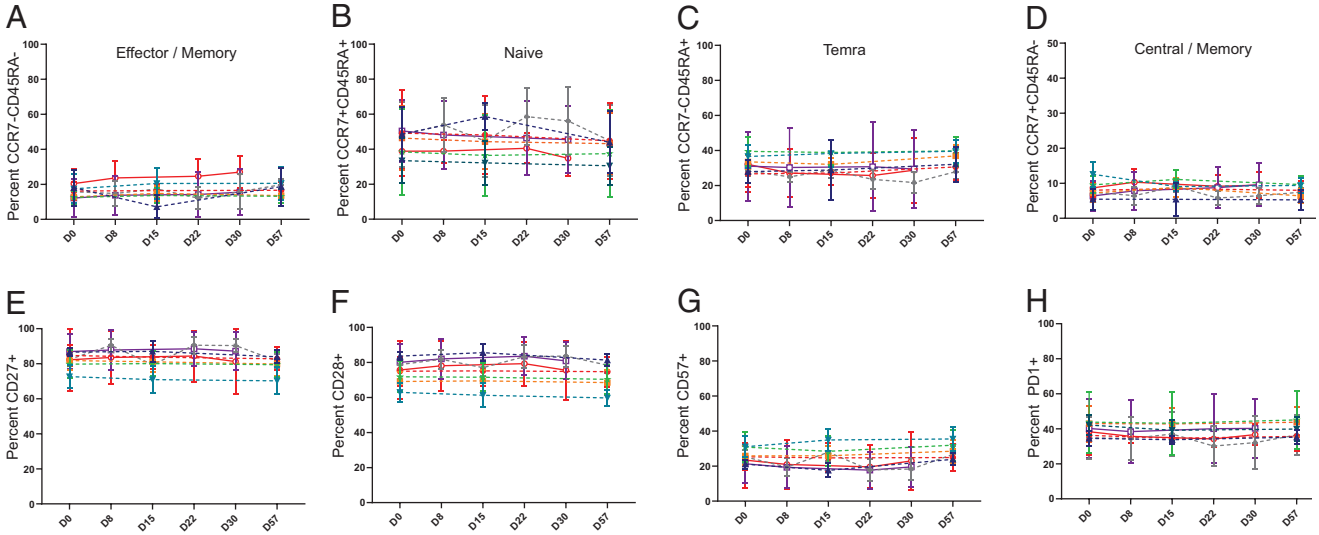

FIGURE 3. Frequencies of CD8 subpopulations of T cells, as indicated. (**A**–**H**) CD8 subpopulations. Symbols refer to the groups defined in Fig. 2A, and data are means ± SEM of $n = 3–6$ subjects.

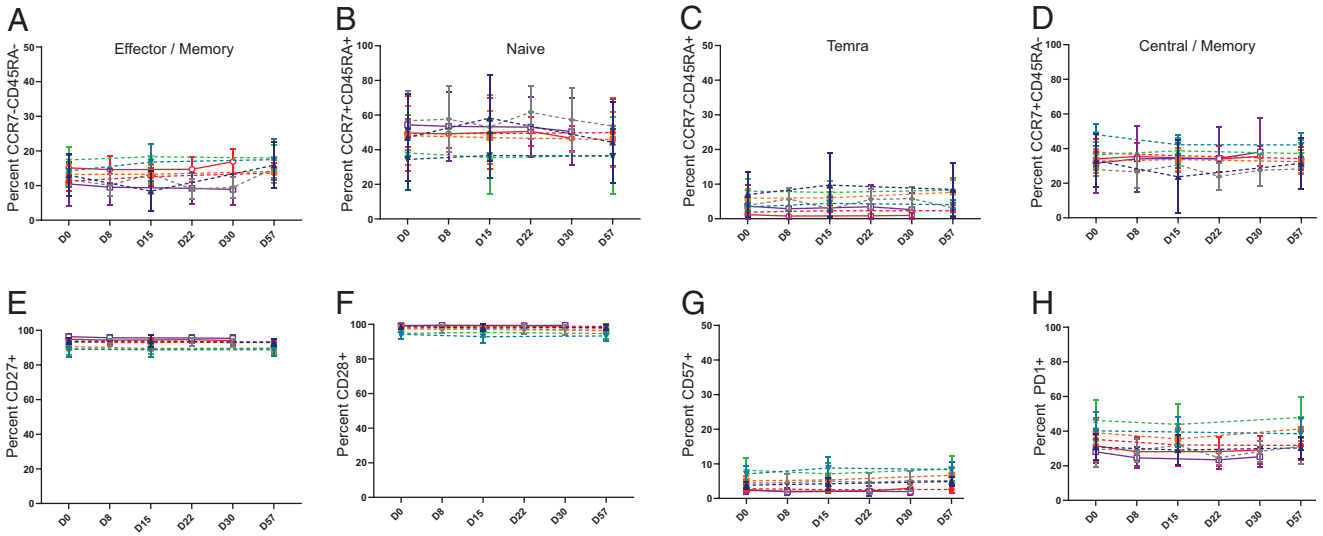

FIGURE 4. Frequencies of CD4 subpopulations of T cells, as indicated. (**A**–**H**) CD8 subpopulations. Symbols refer to the groups defined in Fig. 2A, and data are means ± SEM of $n = 3$–6 subjects.

T cells (Fig. 6). These results illustrate in humans the expected biological effect of OSE-127 with a complete blockade of IL-7 consumption by T cells achieved by a ≥0.2 mg/kg single i.v. dose.

Dose-dependent transcriptomic modifications

As previously described (44), IL-7 signaling in human PBMCs induces rapid transcriptomic modifications within a few hours and the expression of a distinct transcriptomic landscape that can be detected by RNA-seq. These 45 upregulated and 11 downregulated genes in IL-7–stimulated samples compared with the unstimulated samples were selected as genes of interest with an absolute fold change >1 and a Benjamini–Hochberg-adjusted p value <5% (Fig. 7A, 7B) and used to calculate an IL-7 ssGSEA signature (IL-7–induced signature). RNA-seq analysis of PBMCs before (day 0) and after treatment (day 15) showed that the IL-7–induced gene signature is significantly decreased in subjects who received 10 mg/kg OSE-127 whereas no change was observed in the placebo group (Fig. 7C). A differential gene expression signature performed before and after OSE-127 treatment identified 41 significantly and differentially expressed genes; among them, six (*BCL2*, *CISH*, *PTGER2*, *DPP4*, *SOCS2*, and *FLT3LG*)

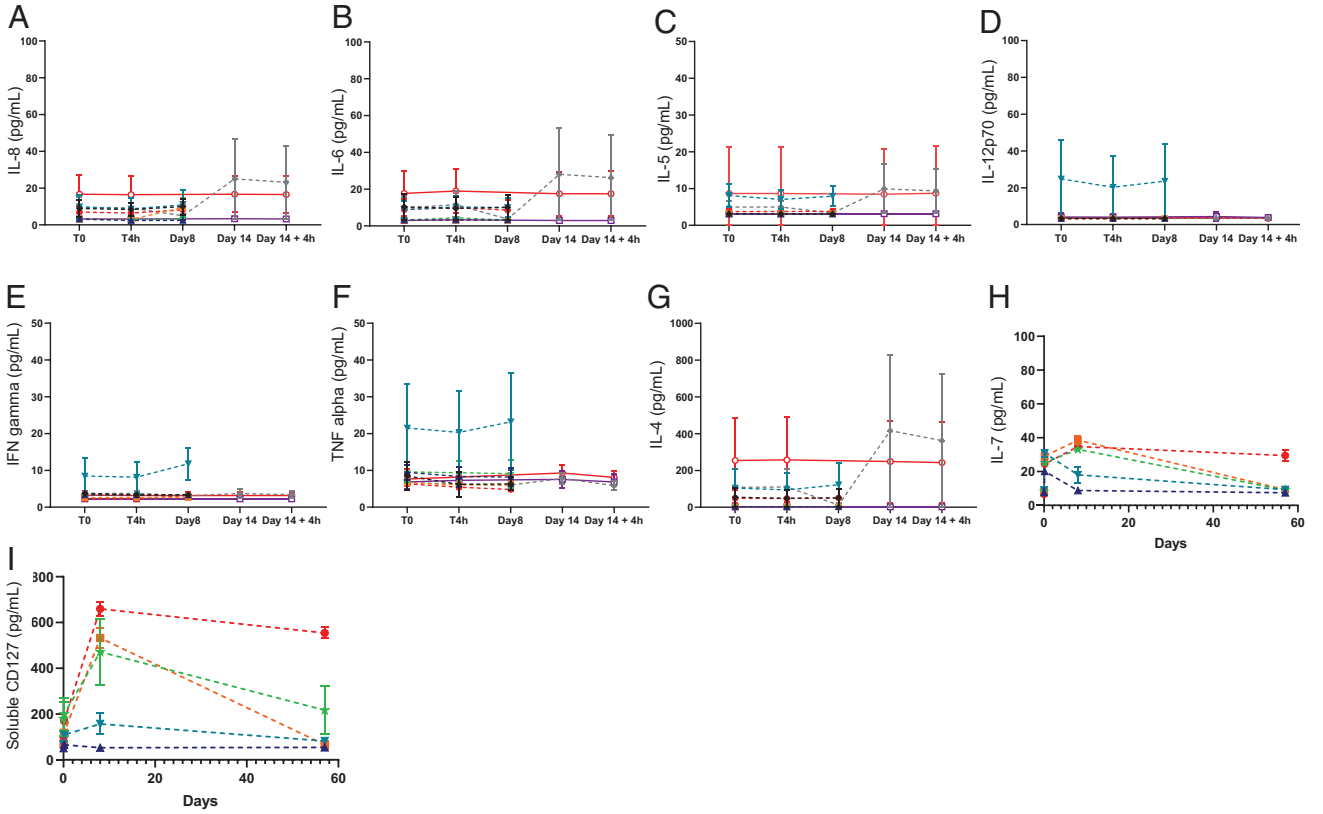

FIGURE 5. Cytokine and soluble CD127 levels in the serum of healthy volunteers, as indicated. (**A**–**H**) Cytokines. (**I**) Soluble CD127. Symbols refer to the groups defined in Fig. 2A, and data are means ± SEM of $n = 3$–6 subjects.

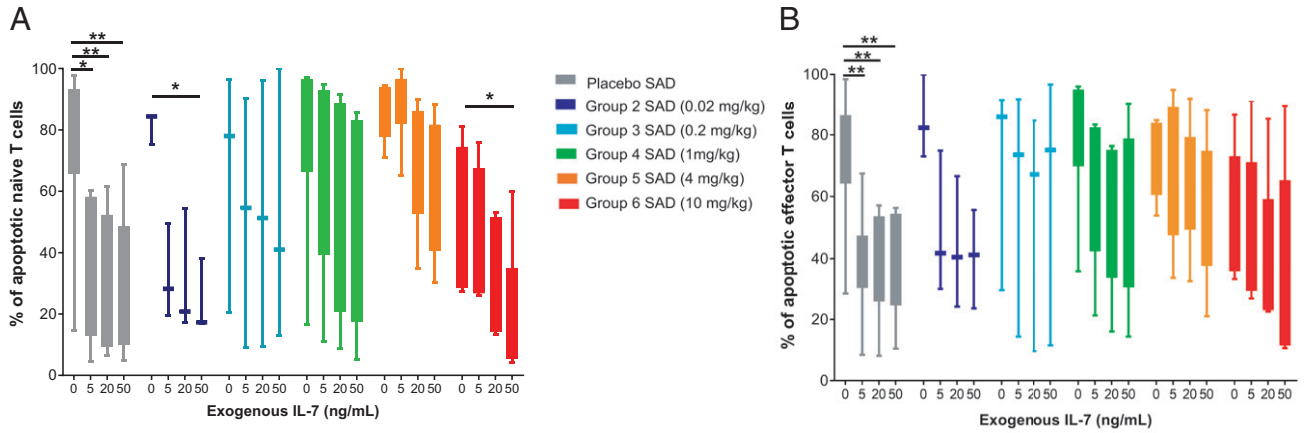

FIGURE 6. Ex vivo response to IL-7 treatment. (**A** and **B**) IL-7 induced rescue from apoptosis measured in (A) naive and (B) effector T lymphocytes isolated from treated subjects, as indicated. Data are means ± SEM of $n = 3–6$ subjects. *$p < 0.05$, **$p < 0.01$.

were inversely and significantly modulated by IL-7 when overlapping signatures (Fig. 7D). This small six-gene signature alone was sufficient and significantly differentially expressed in PBMCs isolated from the group of 10 mg/kg OSE-127 at day 15 compared with day 1 (predose), whereas no modification was observed in the placebo group (Fig. 7C–E). Interestingly, the decrease of this six-gene signature was sustained overtime as illustrated by samples analyzed at day 57 (Fig. 7F), in accordance with drug exposure in this group. The differential expression of four of these six genes (*BCL2*, *CISH*, *PTGER2*, and *DPP4*) has been individually validated by quantitative RT-PCR (Supplemental Fig. 2A–D). Interestingly, this novel four-gene signature appears to follow a dose-dependent expression, as assessed by quantitative PCR (qPCR) (Supplemental Fig. 2E). Altogether, these data indicate that qPCR monitoring of *BCL2*, *CISH*,

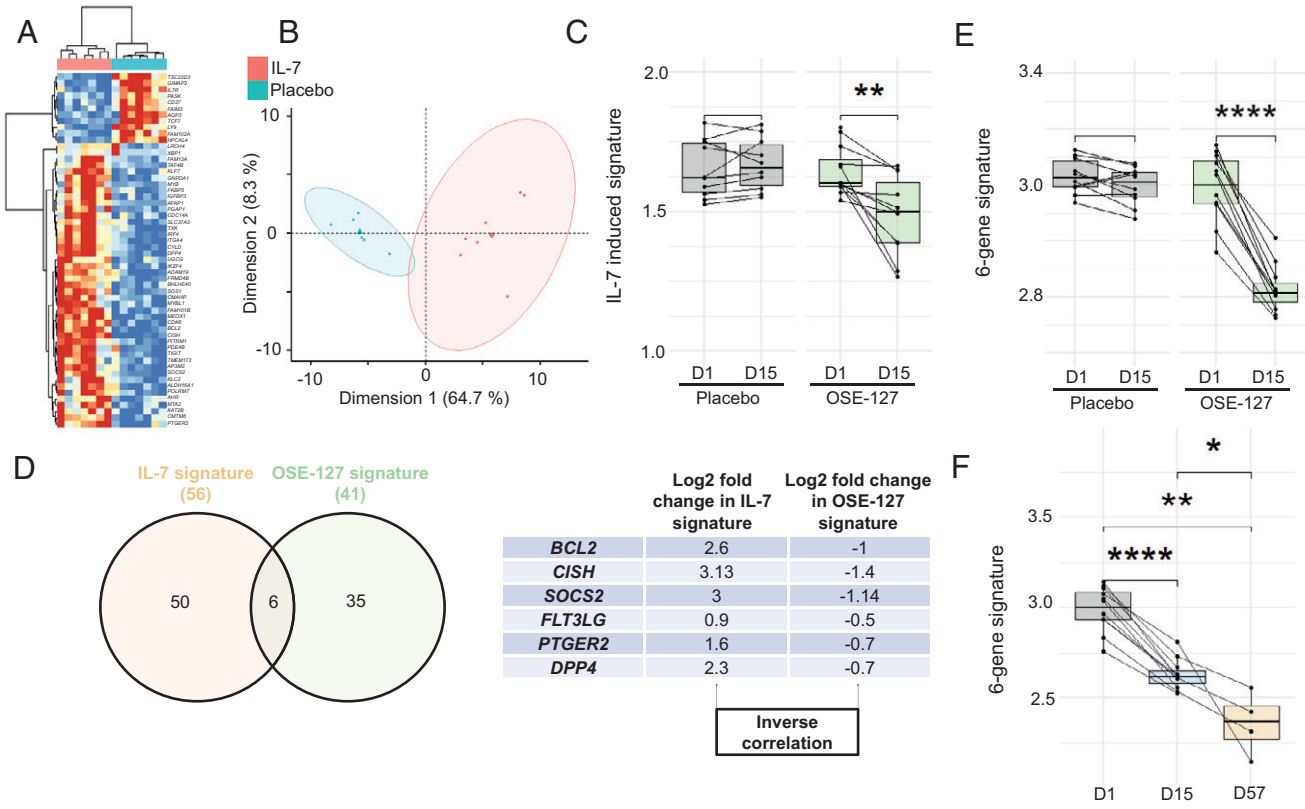

FIGURE 7. In silico monitoring of OSE-127 activity. (**A**) Hierarchical clustering and (**B**) principal component analysis representation of the 45 genes upregulated and 11 genes downregulated following IL-7 stimulation of PBMCs and used as ssGSEA signature. (**C**) ssGSEA IL-7–induced signature expression in placebo-treated and OSE-127–treated (10 mg/kg) healthy volunteers. (**D**) Cross-validation of the six genes differentially expressed in PBMCs stimulated with IL-7 and the PBMCs from healthy volunteers of the OSE-127 phase I study. (**E**) ssGSEA six-gene signature on days 1 and 15 expressed by PBMCs from healthy donors treated with OSE-127 at 10 mg/kg or placebo. (**F**) ssGSEA six-gene signature related to OSE-127 product follow-up on PBMCs from healthy volunteers treated with OSE-127 (10 mg/kg) as indicated. *$p < 0.05$, **$p < 0.01$, ****$p < 0.0001$.

PTGER2, and *DPP4* expression in blood cells represents a robust and simple means to monitor the biological activity of OSE-127 in silico and that IL-7–induced gene expression modification is significantly inhibited in vivo at single i.v. doses ≥1 mg/kg.

Discussion

This trial represents the first administration of OSE-127 to humans, a humanized IgG4 mAb raised against CD127. OSE-127 administration was well tolerated at all doses tested and not associated with peripheral cytokine release or with significant lymphopenia or significant peripheral T cell subtype modification.

In previous attempts to target IL-7R using anti-CD127 mAbs (GSK2618960 and PF-06342674/RN168), clinical developments were stopped and/or complicated by high immunogenicity levels after dosing in humans (41, 42), limiting the possibility to explore clinical efficacy of IL-7/IL-7R pathway selective inhibition. We previously reported that, depending on the epitope, several antagonistic anti-CD127 mAbs share a degree of paradoxical agonistic activity associated with receptor internalization, downstream signaling different from the JAK-STAT pathway, and subsequent transcriptomic leukocyte modification (44). In contrast to GSK2618960 and PF-06342674 targeting the site 1 only epitope and triggering receptor internalization (44, 46, 52), OSE-127 binds site 1 and site 2b of CD127, thereby preventing the heterodimerization with common γ-chain, and it does not induce receptor internalization with subsequent agonist activity on IL-7R signaling in preclinical studies (44). Furthermore, although GSK2618960 and PF-06342674 are anti-CD127 mAbs of IgG1 isotypes, an IgG4 isotype was chosen to design OSE-127 (bearing the S228P hinge mutation to prevent Fab-arm exchange [45]) to abolish Fc-mediated effector functions and to avoid T cell depletion through complement-dependent cytotoxicity or Ab-dependent cellular cytotoxicity.

OSE-127 administrations were well tolerated, there was no safety concern, and all TEAEs reported were only of grades 1 or 2 in severity, with no remarkable difference or dose-dependent trend in adverse event incidence between the several OSE-127 doses and placebo. Of note, the maximal doses administered twice in two subjects of the 10 mg/kg dose level group were 857 and 847 mg with no safety concerns. The PK was nonlinear at low doses as anticipated with target-mediated drug disposition, but with typical terminal elimination half-life for therapeutics mAbs, from 4.6 to 11.7 d over the range of 1–10 mg/kg single injection and up to 16 d after a second dose at 10 mg/kg. This contrasts with the rapid elimination observed with previous anti-CD127 mAbs, suggesting that Ab-induced receptor internalization was associated with accelerated drug elimination: $t_{1/2}$ = 2.7 d at 3 mg/kg every 2 wk and 3.5 d at 8 mg/kg every 2 wk for PF-06342674/RN168 (42) and $t_{1/2}$ = 2.4 d at 0.6 mg/kg and 5.1 d at 2 mg/kg for GSK2618960 (41). Complete RO (>95%) has been measured in peripheral blood with longer duration with higher doses (up to 30 and 50 d with 4 and 10 mg/kg single doses, respectively) in accordance with increased PK drug exposure at higher doses. No significant decrease in blood leukocytes or T lymphocytes has been observed or any significant alteration of T cell subtype frequencies despite high drug exposure and full RO over up to 80 d with double 10 mg/kg administrations. This confirms our previous preclinical observations in nonhuman primates (44, 53) and sharply contrasts with previous rodent studies using anti-CD127 mAbs, which induced profound lymphodepletion within a few weeks of therapy (23, 24, 38, 54), suggesting important IL-7 biological differences between humans/primates and rodents. However, other factors, such as choice of isotype with and without effector functions, may participate significantly in the T cell decrease observed with some anti-CD127 mAbs. Indeed, complete RO for 3 mo in type 1 diabetes with PF-06342674/RN168 led to a significant decline of both naive (−40%) and memory (−70%) $CD4^+$ and $CD8^+$ T cells (42). Whereas ratios of Tregs to $CD4^+$ or to CD8 effectors were increased versus baseline, the absolute number of Tregs also declined (−50%) at all doses after a month of treatment. PF-06342674 was estimated to have 20-fold more potent inhibitory effect on T effector memory cells relative to Tregs, resulting in a nonmonotonic and bell-shaped curve dose-response relationship for the Treg/T effector memory ratio, thus complexifying clinical development and dose/regimen selection (55). Our opposite observation (compared with PF-06342674/RN168 and GSK2618960) using the fully antagonist IgG4 OSE-127 Ab at high doses with confirmed target engagement and decrease of IL-7–induced gene expression indicates that the T cell decline observed with previous anti-CD127 mAbs may not solely be explained by IL-7 cytokine deprivation. RO has been maintained for only 3 wk with GSK2618960 due to high immunogenicity, limiting the interpretation of this anti-CD127 mAb on longer IL-7 deprivation signals and T cell numbers in healthy volunteers (41).

CD127 receptor expression on peripheral blood T lymphocytes was stable over time after administration of OSE-127 from low to high doses, thus confirming the absence of Ab-induced IL-7R internalization in humans, in contrast to previous anti-CD127 mAbs targeting site 1 only (46, 52). ADAs, when present, were apparent in subjects only after OSE-127 being eliminated from the plasma. Of course, drug tolerance may interfere with the assay, and thus it is difficult to estimate the effect of ADAs on PK/PD parameters, even though no difference was observed in PK or PD parameters between individuals with and without detectable ADAs. This finding supports the view that no PK/PD-impacting and neutralizing ADAs were generated through the present trial. However, this observation also contrasts with previous site 1–only internalizing anti-CD127 mAbs: GSK2618960 injection in healthy volunteers led to persistent and neutralizing ADAs appearing after 3 wk in 83 and 100% of subjects administered 0.6 and 2 mg/kg, respectively (41). Although no results were posted or published to our knowledge with PF-06342674/RN168 phase I in healthy volunteers of NCT01740609, of the 30 type 1 diabetes patients treated with PF-06342674/RN168, 73.3% developed ADAs, of which 54.5% were neutralizing (42). PF-06342674/RN168 evaluation in multiple sclerosis was prematurely terminated by the company, but the posted results of the clinical trial (NCT02045732) indicated that three of three subjects administered 0.25 mg/kg of PF-06342674 developed ADAs. Further investigation revealed the presence of GSK2618960-specific memory B cells in the blood after treatment, indicating the development of immunological memory for these persistent ADA responses (52). Ex vivo exploration showed that the human dendritic cell subset treated with GSK2618960 exhibited enhanced activation and that unintended receptor-mediated internalization, subsequent agonist activity, and enhanced Ag processing and presentation by dendritic cells (56, 57) were the main risk factors contributing to the robust clinical immunogenicity, as concluded by the authors.

Despite the absence of changes in lymphocyte subset counts and frequencies and surface markers, the biological activity of OSE-127 could be captured at the transcriptomic level. Assessment of the biological target-engagement potential of OSE-127 in healthy volunteers has been made possible by RNA-seq of peripheral leukocytes over time compared with baseline and cross-analysis with IL-7–induced gene expression signature upon in vitro stimulation on independent healthy blood donors not exposed to anti-CD127 mAb (44). A dose- and time-dependent effect has been observed on the expression of four IL-7 pathway–related genes, inversely correlated upon exposure to IL-7 or OSE-127 and associated with the biological effect of IL-7 such as the *BCL2* antiapoptotic gene (58–60) or the negative regulator of cytokine signaling *CISH* (61). Thus, qPCR monitoring of the expression of only four genes (*BCL2*, *CISH*, *PTGER2*, and *DPP4*) in peripheral blood cells represents a robust and simple means to

monitor the biological activity of OSE-127 in vivo. Peripheral blood T cell transcriptome RNA-seq analysis before and after treatment with PF-06342674/RN168 in type 1 diabetes also identified signaling molecules associated with T cell survival such as *BCL2* (42), confirming the unceasing biological role of IL-7 in regulating T cell apoptosis in both steady state and inflammatory pathogenic settings. Finally, OSE-127 did not significantly alter total lymphocyte counts, T cell phenotype, or lymphocyte subset frequencies. Given that IL-7R may also regulate migration of primed T cells to target tissues (13, 14), these data, together with absence of internalization, cytokine release, and opposite transcriptomic modification induced by IL-7, reinforce the purely antagonistic activity of OSE-127 in human. It is noteworthy that the ethnicity of all participants were white, and therefore all results may not be transferable to other ethnicities. Further clinical experience will confirm whether potential theoretical risks such as decreased lymphocyte count or infusion-related reactions are reported with prolonged treatment with OSE-127 in patient populations.

In conclusion, to our knowledge, this is the first study to evaluate the safety, PK, and PD of OSE-127 in healthy subjects. The presented data provide evidence that IL-7R can be safely and efficiently blocked with an appropriately designed mAb targeting CD127 without inducing serious adverse events or target internalization and downstream agonist signaling. These findings strongly support further clinical development of OSE-127, and two phase II clinical trials are currently ongoing in ulcerative colitis (CoTikiS study: NCT04882007) and in primary Sjögren's syndrome (NCT04605978). Further indications where the IL-7 pathway is involved (1) will be investigated.

Disclosures

F.C., R.A., L.B., G.T., I.B., C.M., C.F., I.G., S. Pengam, E.S., F.D.S., J.-P.C., D.C., and N.P. are employees and shareholders of OSE Immunotherapeutics, a company owning OSE-127 anti–IL-7Ra antagonist mAb. L.B., C.M., I.B., S. Pengam, I.G., and N.P are authors of patents related to anti–IL-7Ra antagonist mAb. S. Poli is an advisor. The other authors have no financial conflicts of interest.

References

1. Dooms, H. 2013. Interleukin-7: fuel for the autoimmune attack. *J. Autoimmun.* 45: 40–48.
2. Carrette, F., and C. D. Surh. 2012. IL-7 signaling and CD127 receptor regulation in the control of T cell homeostasis. *Semin. Immunol.* 24: 209–217.
3. Mazzucchelli, R., and S. K. Durum. 2007. Interleukin-7 receptor expression: intelligent design. *Nat. Rev. Immunol.* 7: 144–154.
4. Mackall, C. L., T. J. Fry, and R. E. Gress. 2011. Harnessing the biology of IL-7 for therapeutic application. *Nat. Rev. Immunol.* 11: 330–342.
5. Sercan Alp, Ö., S. Durlanik, D. Schulz, M. McGrath, J. R. Grün, M. Bardua, K. Ikuta, E. Sgouroudis, R. Riedel, S. Zehentmeier, et al. 2015. Memory $CD8^+$ T cells colocalize with $IL\text{-}7^+$ stromal cells in bone marrow and rest in terms of proliferation and transcription. *Eur. J. Immunol.* 45: 975–987.
6. Schluns, K. S., W. C. Kieper, S. C. Jameson, and L. Lefrançois. 2000. Interleukin-7 mediates the homeostasis of naïve and memory CD8 T cells in vivo. *Nat. Immunol.* 1: 426–432.
7. Cieri, N., B. Camisa, F. Cocchiarella, M. Forcato, G. Oliveira, E. Provasi, A. Bondanza, C. Bordignon, J. Peccatori, F. Ciceri, et al. 2013. IL-7 and IL-15 instruct the generation of human memory stem T cells from naive precursors. *Blood* 121: 573–584.
8. Cui, G., M. M. Staron, S. M. Gray, P.-C. Ho, R. A. Amezquita, J. Wu, and S. M. Kaech. 2015. IL-7-induced glycerol transport and TAG synthesis promotes memory $CD8^+$ T cell longevity. *Cell* 161: 750–761.
9. Kondrack, R. M., J. Harbertson, J. T. Tan, M. E. McBreen, C. D. Surh, and L. M. Bradley. 2003. Interleukin 7 regulates the survival and generation of memory CD4 cells. *J. Exp. Med.* 198: 1797–1806.
10. Kieper, W. C., J. T. Tan, B. Bondi-Boyd, L. Gapin, J. Sprent, R. Ceredig, and C. D. Surh. 2002. Overexpression of interleukin (IL)-7 leads to IL-15-independent generation of memory phenotype $CD8^+$ T cells. *J. Exp. Med.* 195: 1533–1539.
11. Yamaki, S., S. Ine, T. Kawabe, Y. Okuyama, N. Suzuki, P. Soroosh, S. F. Mousavi, H. Nagashima, S. L. Sun, T. So, et al. 2014. OX40 and IL-7 play synergistic roles in the homeostatic proliferation of effector memory $CD4^+$ T cells. *Eur. J. Immunol.* 44: 3015–3025.
12. Mehrotra, P. T., A. J. Grant, and J. P. Siegel. 1995. Synergistic effects of IL-7 and IL-12 on human T cell activation. *J. Immunol.* 154: 5093–5102.
13. Belarif, L., R. Danger, L. Kermarrec, V. Nerrière-Daguin, S. Pengam, T. Durand, C. Mary, E. Kerdreux, V. Gauttier, A. Kucik, et al. 2019. IL-7 receptor influences anti-TNF responsiveness and T cell gut homing in inflammatory bowel disease. *J. Clin. Invest.* 129: 1910–1925.
14. Cimbro, R., L. Vassena, J. Arthos, C. Cicala, J. H. Kehrl, C. Park, I. Sereti, M. M. Lederman, A. S. Fauci, and P. Lusso. 2012. IL-7 induces expression and activation of integrin α4β7 promoting naive T-cell homing to the intestinal mucosa. *Blood* 120: 2610–2619.
15. Bikker, A., A. A. Kruize, K. M. G. van der Wurff-Jacobs, R. P. Peters, M. Kleinjan, F. Redegeld, W. de Jager, F. P. J. G. Lafeber, and J. A. G. van Roon. 2014. Interleukin-7 and Toll-like receptor 7 induce synergistic B cell and T cell activation. *PLoS One* 9: e94756.
16. Rochman, Y., R. Spolski, and W. J. Leonard. 2009. New insights into the regulation of T cells by γ_c family cytokines. *Nat. Rev. Immunol.* 9: 480–490.
17. Walsh, S. T. R. 2012. Structural insights into the common γ-chain family of cytokines and receptors from the interleukin-7 pathway. *Immunol. Rev.* 250: 303–316.
18. McElroy, C. A., P. J. Holland, P. Zhao, J.-M. Lim, L. Wells, E. Eisenstein, and S. T. R. Walsh. 2012. Structural reorganization of the interleukin-7 signaling complex. *Proc. Natl. Acad. Sci. USA* 109: 2503–2508.
19. Crawley, A. M., A. Vranjkovic, E. Faller, M. McGuinty, A. Busca, S. C. Burke, S. Cousineau, A. Kumar, P. A. Macpherson, and J. B. Angel. 2014. Jak/STAT and PI3K signaling pathways have both common and distinct roles in IL-7-mediated activities in human $CD8^+$ T cells. *J. Leukoc. Biol.* 95: 117–127.
20. He, R., and R. S. Geha. 2010. Thymic stromal lymphopoietin. *Ann. N. Y. Acad. Sci.* 1183: 13–24.
21. Liu, W., A. L. Putnam, Z. Xu-Yu, G. L. Szot, M. R. Lee, S. Zhu, P. A. Gottlieb, P. Kapranov, T. R. Gingeras, B. Fazekas de St. Groth, et al. 2006. CD127 expression inversely correlates with FoxP3 and suppressive function of human $CD4^+$ T reg cells. *J. Exp. Med.* 203: 1701–1711.
22. Barata, J. T., S. K. Durum, and B. Seddon. 2019. Flip the coin: IL-7 and IL-7R in health and disease. *Nat. Immunol.* 20: 1584–1593.
23. Willis, C. R., A. Seamons, J. Maxwell, P. M. Treuting, L. Nelson, G. Chen, S. Phelps, C. L. Smith, T. Brabb, B. M. Iritani, and L. Maggio-Price. 2012. Interleukin-7 receptor blockade suppresses adaptive and innate inflammatory responses in experimental colitis. *J. Inflamm. (Lond.)* 9: 39.
24. Lee, L.-F., K. Logronio, G. H. Tu, W. Zhai, I. Ni, L. Mei, J. Dilley, J. Yu, A. Rajpal, C. Brown, et al. 2012. Anti-IL-7 receptor-α reverses established type 1 diabetes in nonobese diabetic mice by modulating effector T-cell function. [Published erratum appears in 2012 *Proc. Natl. Acad. Sci. USA* 109: 16393.] *Proc. Natl. Acad. Sci. USA* 109: 12674–12679.
25. Penaranda, C., W. Kuswanto, J. Hofmann, R. Kenefeck, P. Narendran, L. S. K. Walker, J. A. Bluestone, A. K. Abbas, and H. Dooms. 2012. IL-7 receptor blockade reverses autoimmune diabetes by promoting inhibition of effector/memory T cells. *Proc. Natl. Acad. Sci. USA* 109: 12668–12673.
26. Hartgring, S. A. Y., C. R. Willis, D. Alcorn, L. J. Nelson, J. W. J. Bijlsma, F. P. J. G. Lafeber, and J. A. G. van Roon. 2010. Blockade of the interleukin-7 receptor inhibits collagen-induced arthritis and is associated with reduction of T cell activity and proinflammatory mediators. *Arthritis Rheum.* 62: 2716–2725.
27. van Roon, J. A. G., K. A. Glaudemans, J. W. Bijlsma, and F. P. Lafeber. 2003. Interleukin 7 stimulates tumour necrosis factor α and Th1 cytokine production in joints of patients with rheumatoid arthritis. *Ann. Rheum. Dis.* 62: 113–119.
28. van Roon, J. A. G., M. C. Verweij, M. W. Wijk, K. M. G. Jacobs, J. W. J. Bijlsma, and F. P. J. G. Lafeber. 2005. Increased intraarticular interleukin-7 in rheumatoid arthritis patients stimulates cell contact-dependent activation of $CD4^+$ T cells and macrophages. *Arthritis Rheum.* 52: 1700–1710.
29. Bonifati, C., E. Trento, P. Cordiali-Fei, M. Carducci, A. Mussi, L. D'Auria, F. Pimpinelli, M. Fazio, and F. Ameglio. 1997. Increased interleukin-7 concentrations in lesional skin and in the sera of patients with plaque-type psoriasis. *Clin. Immunol. Immunopathol.* 83: 41–44.
30. Bikker, A., A. A. Kruize, M. Wenting, M. A. Versnel, J. W. J. Bijlsma, F. P. J. G. Lafeber, and J. A. G. van Roon. 2012. Increased interleukin (IL)-7Rα expression in salivary glands of patients with primary Sjögren's syndrome is restricted to T cells and correlates with IL-7 expression, lymphocyte numbers and activity. *Ann. Rheum. Dis.* 71: 1027–1033.
31. Jin, J.-O., T. Kawai, S. Cha, and Q. Yu. 2013. Interleukin-7 enhances the Th1 response to promote the development of Sjögren's syndrome-like autoimmune exocrinopathy in mice. *Arthritis Rheum.* 65: 2132–2142.
32. Akkapeddi, P., R. Fragoso, J. A. Hixon, A. S. Ramalho, M. L. Oliveira, T. Carvalho, A. Gloger, M. Matasci, F. Corzana, S. K. Durum, et al. 2019. A fully human anti-IL-7Rα antibody promotes antitumor activity against T-cell acute lymphoblastic leukemia. *Leukemia* 33: 2155–2168.
33. Abdelrasoul, H., A. Vadakumchery, M. Werner, L. Lenk, A. Khadour, M. Young, O. El Ayoubi, F. Vogiatzi, M. Krämer, V. Schmid, et al. 2020. Synergism between IL7R and CXCR4 drives BCR-ABL induced transformation in Philadelphia chromosome-positive acute lymphoblastic leukemia. *Nat. Commun.* 11: 3194.
34. Alsadeq, A., L. Lenk, A. Vadakumchery, A. Cousins, C. Vokuhl, A. Khadour, F. Vogiatzi, F. Seyfried, L.-H. Meyer, G. Cario, et al. 2018. IL7R is associated with CNS infiltration and relapse in pediatric B-cell precursor acute lymphoblastic leukemia. *Blood* 132: 1614–1617.
35. Almeida, A. R. M., J. L. Neto, A. Cachucho, M. Euzébio, X. Meng, R. Kim, M. B. Fernandes, B. Raposo, M. L. Oliveira, D. Ribeiro, et al. 2021. Interleukin-7 receptor α mutational activation can initiate precursor B-cell acute lymphoblastic leukemia. *Nat. Commun.* 12: 7268.
36. Silva, A., A. R. M. Almeida, A. Cachucho, J. L. Neto, S. Demeyer, M. de Matos, T. Hogan, Y. Li, J. Meijerink, J. Cools, et al. 2021. Overexpression of wild-type IL-7Rα promotes T-cell acute lymphoblastic leukemia/lymphoma. *Blood* 138: 1040–1052.

37. Kreft, K. L., E. Verbraak, A. F. Wierenga-Wolf, M. van Meurs, B. A. Oostra, J. D. Laman, and R. Q. Hintzen. 2012. The IL-7Rα pathway is quantitatively and functionally altered in CD8 T cells in multiple sclerosis. *J. Immunol.* 188: 1874–1883.
38. Lee, L.-F., R. Axtell, G. H. Tu, K. Logronio, J. Dilley, J. Yu, M. Rickert, B. Han, W. Evering, M. G. Walker, et al. 2011. IL-7 promotes T_H1 development and serum IL-7 predicts clinical response to interferon-β in multiple sclerosis. *Sci. Transl. Med.* 3: 93ra68.
39. Hafler, D. A., A. Compston, S. Sawcer, E. S. Lander, M. J. Daly, P. L. De Jager, P. I. de Bakker, S. B. Gabriel, D. B. Mirel, A. J. Ivinson, et al.; International Multiple Sclerosis Genetics Consortium. 2007. Risk alleles for multiple sclerosis identified by a genomewide study. *N. Engl. J. Med.* 357: 851–862.
40. Todd, J. A., N. M. Walker, J. D. Cooper, D. J. Smyth, K. Downes, V. Plagnol, R. Bailey, S. Nejentsev, S. F. Field, F. Payne, et al. 2007. Robust associations of four new chromosome regions from genome-wide analyses of type 1 diabetes. *Nat. Genet.* 39: 857–864.
41. Ellis, J., A. van Maurik, L. Fortunato, S. Gisbert, K. Chen, A. Schwartz, S. McHugh, A. Want, S. Santos Franco, J. J. Oliveira, et al. 2019. Anti-IL-7 receptor α monoclonal antibody (GSK2618960) in healthy subjects—a randomized, double-blind, placebo-controlled study. *Br. J. Clin. Pharmacol.* 85: 304–315.
42. Herold, K. C., S. L. Bucktrout, X. Wang, B. W. Bode, S. E. Gitelman, P. A. Gottlieb, J. Hughes, T. Joh, J. B. McGill, J. H. Pettus, et alRN168 Working Group. 2019. Immunomodulatory activity of humanized anti-IL-7R monoclonal antibody RN168 in subjects with type 1 diabetes. *JCI Insight* 4: e126054.
43. Hixon, J. A., C. Andrews, L. Kashi, C. L. Kohnhorst, E. Senkevitch, K. Czarra, J. T. Barata, W. Li, J. P. Schneider, S. T. R. Walsh, and S. K. Durum. 2020. New anti-IL-7Rα monoclonal antibodies show efficacy against T cell acute lymphoblastic leukemia in pre-clinical models. *Leukemia* 34: 35–49.
44. Belarif, L., C. Mary, L. Jacquemont, H. L. Mai, R. Danger, J. Hervouet, D. Minault, V. Thepenier, V. Nerrière-Daguin, E. Nguyen, et al. 2018. IL-7 receptor blockade blunts antigen-specific memory T cell responses and chronic inflammation in primates. *Nat. Commun.* 9: 4483.
45. Silva, J.-P., O. Vetterlein, J. Jose, S. Peters, and H. Kirby. 2015. The S228P mutation prevents in vivo and in vitro IgG4 Fab-arm exchange as demonstrated using a combination of novel quantitative immunoassays and physiological matrix preparation. *J. Biol. Chem.* 290: 5462–5469.
46. Kern, B., W. Li, C. Bono, L.-F. Lee, and E. Kraynov. 2016. Receptor occupancy and blocking of STAT5 signaling by an anti-IL-7 receptor α antibody in cynomolgus monkeys. *Cytometry B Clin. Cytom.* 90: 191–198.
47. Rivière, E., J. Pascaud, A. Virone, A. Dupré, B. Ly, A. Paoletti, R. Seror, N. Tchitchek, M. Mingueneau, N. Smith, et al. 2021. Interleukin-7/interferon axis drives T cell and salivary gland epithelial cell interactions in Sjögren's syndrome. *Arthritis Rheumatol.* 73: 631–640.
48. Braudeau, C., N. Salabert-Le Guen, J. Chevreuil, M. Rimbert, J. C. Martin, and R. Josien. 2021. An easy and reliable whole blood freezing method for flow cytometry immuno-phenotyping and functional analyses. *Cytometry B Clin. Cytom.* 100: 652–665.
49. Hänzelmann, S., R. Castelo, and J. Guinney. 2013. GSVA: gene set variation analysis for microarray and RNA-seq data. *BMC Bioinformatics* 14: 7.
50. Barbie, D. A., P. Tamayo, J. S. Boehm, S. Y. Kim, S. E. Moody, I. F. Dunn, A. C. Schinzel, P. Sandy, E. Meylan, C. Scholl, et al. 2009. Systematic RNA interference reveals that oncogenic KRAS-driven cancers require TBK1. *Nature* 462: 108–112.
51. Nishimoto, N., K. Terao, T. Mima, H. Nakahara, N. Takagi, and T. Kakehi. 2008. Mechanisms and pathologic significances in increase in serum interleukin-6 (IL-6) and soluble IL-6 receptor after administration of an anti-IL-6 receptor antibody, tocilizumab, in patients with rheumatoid arthritis and Castleman disease. *Blood* 112: 3959–3964.
52. Liao, K., K. Chen, S. Brett, A. Gehman, A. M. Schwartz, G. R. Gunn, and S. L. DeWall. 2021. Characterization of the robust humoral immune response to GSK2618960, a humanized anti-IL-7 receptor monoclonal antibody, observed in healthy subjects in a phase 1 study. *PLoS One* 16: e0249049.
53. Mai, H. L., T. V. H. Nguyen, J. Branchereau, N. Poirier, K. Renaudin, C. Mary, L. Belarif, D. Minault, J. Hervouet, S. Le Bas-Berdardet, et al. 2020. Interleukin-7 receptor blockade by an anti-CD127 monoclonal antibody in nonhuman primate kidney transplantation. *Am. J. Transplant.* 20: 101–111.
54. Mai, H.-L., F. Boeffard, J. Longis, R. Danger, B. Martinet, F. Haspot, B. Vanhove, S. Brouard, and J.-P. Soulillou. 2014. IL-7 receptor blockade following T cell depletion promotes long-term allograft survival. *J. Clin. Invest.* 124: 1723–1733.
55. Williams, J. H., C. Udata, B. J. Ganguly, S. L. Bucktrout, T. Joh, M. Shannon, G. Y. Wong, M. Levisetti, P. D. Garzone, and X. Meng. 2020. Model-based characterization of the pharmacokinetics, target engagement biomarkers, and immunomodulatory activity of PF-06342674, a humanized mAb against IL-7 receptor-α, in adults with type 1 diabetes. *AAPS J.* 22: 23.
56. Gogolák, P., B. Réthi, G. Hajas, and E. Rajnavölgyi. 2003. Targeting dendritic cells for priming cellular immune responses. *J. Mol. Recognit.* 16: 299–317.
57. Xue, L., T. Hickling, R. Song, J. Nowak, and B. Rup. 2016. Contribution of enhanced engagement of antigen presentation machinery to the clinical immunogenicity of a human interleukin (IL)-21 receptor-blocking therapeutic antibody. *Clin. Exp. Immunol.* 183: 102–113.
58. Akashi, K., M. Kondo, U. von Freeden-Jeffry, R. Murray, and I. L. Weissman. 1997. Bcl-2 rescues T lymphopoiesis in interleukin-7 receptor-deficient mice. *Cell* 89: 1033–1041.
59. Chetoui, N., M. Boisvert, S. Gendron, and F. Aoudjit. 2010. Interleukin-7 promotes the survival of human $CD4^+$ effector/memory T cells by up-regulating Bcl-2 proteins and activating the JAK/STAT signalling pathway. *Immunology* 130: 418–426.
60. Jiang, Q., W. Q. Li, R. R. Hofmeister, H. A. Young, D. R. Hodge, J. R. Keller, A. R. Khaled, and S. K. Durum. 2004. Distinct regions of the interleukin-7 receptor regulate different Bcl2 family members. *Mol. Cell. Biol.* 24: 6501–6513.
61. Yoshimura, A., T. Naka, and M. Kubo. 2007. SOCS proteins, cytokine signalling and immune regulation. *Nat. Rev. Immunol.* 7: 454–465.